

Syntheses, Crystal Structures, and the Phase Transformation of Octacyanometallate-Based Ln^{III}–W^V Bimetallic Assemblies with Two-Dimensional Corrugated Layers

Ai-Hua Yuan,^{*[a,b]} Peter D. Southon,^[a] David J. Price,^[a] Cameron J. Kepert,^{*[a]} Hu Zhou,^[b] and Wen-Yan Liu^[b]

Keywords: Octacyanometallates / Lanthanides / Solid-state structures / Tungsten / Layered compounds / Phase transformation

The reactions between Ln(NO₃)₃·*n*H₂O and (Bu₃NH)₃[W(CN)₈]·H₂O have led to two series of octacyanometallate-based complexes: Ln(H₂O)₅[W(CN)₈] [Ln = La(**1**), Pr(**2**), Nd(**3**), Eu(**4**), Gd(**5**)] and Ln(H₂O)₄[W(CN)₈] [Ln = Ho(**6**), Er(**7**), Tm(**8**), Lu(**9**)]. The crystal structures of **1–9** have two-

dimensional corrugated layers in which the Ln^{III} and W^V centres are linked in an alternating fashion. Thermogravimetric (TG) and powder XRD results reveal the presence of a phase transformation in the Ln^{III}–W^V system with increasing atomic number of the Ln^{III} atoms.

Introduction

In the past few years, [M(CN)₈]^{3–/4–} (M = Mo, W, and Nb) anions have become attractive building blocks that can adopt three different spatial configurations [square antiprism (*D*_{4d}), dodecahedron (*D*_{2d}) and bicapped trigonal prism (*C*_{2v})] depending on their surroundings, such as ligands and other metal ions.^[1] In recent studies, investigations of octacyanometallate-based bimetallic systems has mainly focused on second- and third-row transition metals. The exploration of cyano-bridged 3d–*nd* (*n* = 4 or 5) systems based on [M(CN)₈]^{3–/4–} anions and transition metal cations has resulted in a wide variety of coordination networks from 0D ionic complexes and discrete molecules, 1D chains, 2D layers and 3D networks. Due to their flexible molecular structures, multifarious magnetic properties as varied as those of the hexacyanometallates, such as photo-induced magnetism,^[2] relatively high magnetic phase transition temperature^[3] and single-molecule magnetism,^[4] are observed in octacyanometallate-based assemblies.

Recently, the investigation of octacyanometallate-based bimetallic systems has been extended to the first-row lanthanide ions. As lanthanide ions often have higher coordination numbers, mixed d–f complexes using 4d or 5d metal ions can have very complicated topologies and magnetic behaviours that are different from those of 3d–4f complexes.

A better understanding of the property–structure relationships of such materials relies on the synthesis and evaluation of new lanthanide–transition metal complexes. However, synthesis of complexes containing octacyanometallates and lanthanide ions is challenging due to the tendency of the rare earth metal ions to adopt high coordination numbers and their ability to easily adapt to a given environment. To the best of our knowledge, there are limited examples of octacyano- and lanthanide-based assemblies^[5] to date, and these complexes have presented interesting properties such as long-range magnetic ordering, cooling-rate-dependent ferromagnetism and luminescence.

For the reasons noted above, we have tried to prepare lanthanide-containing octacyanometallate-based bimetallic assemblies using [W(CN)₈]^{3–} and Ln³⁺ as building blocks. In the present work, two series of heterobimetallic 4f–5d complexes, Ln(H₂O)₅[W(CN)₈] [Ln = La(**1**), Pr(**2**), Nd(**3**), Eu(**4**), Gd(**5**)] and Ln(H₂O)₄[W(CN)₈] [Ln = Ho(**6**), Er(**7**), Tm(**8**), Lu(**9**)] have been synthesized and characterized structurally. It should be noted here that TG and powder XRD results revealed the presence of phase transformations in the Ln–W system with increasing atomic number of the Ln^{III} atoms (from La to Lu).

Results and Discussion

Crystal Structures of **1–9**

The structures of **1–9** have been determined by single-crystal X-ray diffraction (Table S1). **1–5** are isostructural, have tetragonal geometries and crystallize in the space group *P4/nmm*, except for **1**, which belongs to *P4/ncc*. The crystal structures of **1–5** consist of 2D cyano-bridged corru-

[a] School of Chemistry, The University of Sydney, Sydney NSW 2006, Australia
E-mail: c.kepert@chem.usyd.edu.au

[b] School of Material Science and Engineering, Jiangsu University of Science and Technology, Zhenjiang 212003, China
E-mail: aihuayuan@163.com

Supporting information for this article is available on the WWW under <http://dx.doi.org/10.1002/ejic.201000320>.

gated layers, in which Ln^{III} and W^V centres are linked in an alternating fashion (Figure 1a). In the structures of **1–5**, the [W(CN)₈] moiety exhibits a slightly distorted dodecahedral geometry (*D*_{2d}) with four bridging and four terminal cyano ligands. The W–C bonds are in the range of 2.132 to 2.168 Å and the W–C1–N1 bonds are nearly linear with angles ranging from 175.3 to 179.0° (Table S2). It is worth noting that half of the coordinated cyanide groups in **2–5** are bidentate, establishing physical links (μ-CN) with neighbouring Ln^{III} centres, while the other half are terminal, exhibiting statistical disorder over two crystallographic positions (occupancy of 50% each) for the uncoordinated nitrogen atom. In the structures of **1–5** the Ln^{III} atom is nine-coordinate, ligated by four cyano nitrogen atoms and five oxygen atoms from five water molecules, {LnN₄O₅}, describing a slightly distorted monocapped square antiprism geometry with the O1 atom in a capping position (Figure 2). The sites of one face are finished by four cyano nitrogen atoms with Ln–N_{cyanide} distances ranging from 2.504 to 2.647 Å, while those of the other face by four oxygen atoms with Ln–O distances ranging from 2.467 to 2.620 Å. Four cyanide bridges are close to linear with bond angles of C1–N1–Ln in the range of 165.3 to 176.7°. The geometry of the Ln atom for **1–5** is different from the tricapped trigonal prism found for related complexes Ln(H₂O)₅[W(CN)₈] (Ln = Sm, Eu, Gd, Tb).^[5f,5j]

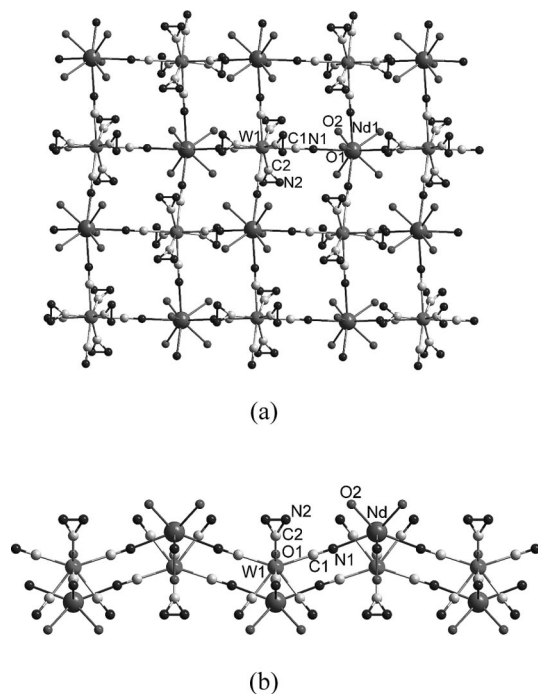


Figure 1. Projection of 2D corrugated layers for **1–5**: (a) in the *ab* plane and (b) along the *c* axis. Note: four terminal cyanide groups in **1** exhibit order, which is different from those in **2–5**.

As shown in Figure 1a, the Ln^{III} and the [W(CN)₈]³⁻ units form 12-membered Ln₂W₂(CN)₄ squares with the Ln^{III} and W^V atoms occupying the vertices. The side view of the 2D corrugated layer is shown in Figure 1b. The average distances of the closest intramolecular Ln^{III}W^V,

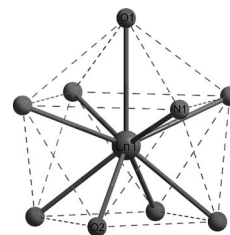


Figure 2. Coordination environment of **1–5**.

Ln^{III}W^V and W^VW^V distances are 5.832, 8.652 and 7.823 Å, respectively. The average Ln^{III}W^V, Ln^{III}Ln^{III} and W^VW^V distances between neighbouring aligned layers are 7.644, 7.123 and 7.123 Å, respectively. The 2D layers are linked by relatively strong O–H⁺–N hydrogen bonds between H₂O molecules and terminal cyano ligands, connecting the O(1 W) coordinated molecules from one layer to the terminal C2N2 cyanide groups of another layer with *d*_{O...N} of 2.781, 2.586, 2.626, 2.606 and 2.614 Å for **1–5**, respectively. It is worth mentioning that the degree of disorder in the structures of complexes **4** and **5** is superior to that of those reported in the literature.^[5f]

Similar to **1–5**, the structures of **6–9** are tetragonal and crystallize in the space group *P4/nmm*. The crystal structures consist of 2D cyano-bridged corrugated layers in which Ln^{III} and W^V ions are linked in an alternating fashion (Figure 3a). The side view of the 2D corrugated layer is shown in Figure 3b. The central geometry around W^V adopts a slightly distorted dodecahedral geometry (*D*_{2d}). The W^V atom is coordinated by eight CN groups, four of which are bridging and four are terminal. For **6–9** the

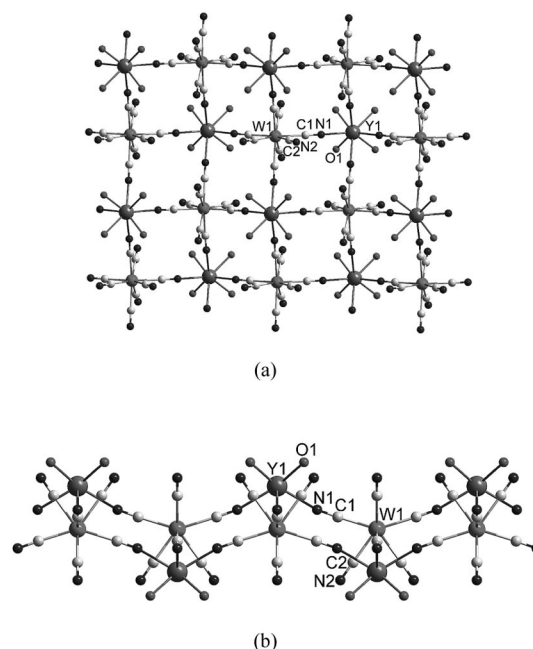


Figure 3. Projection of 2D corrugated layers for **6–9**: (a) in the *ab* plane and (b) along the *c* axis.

average W–C bond length is 2.167 Å and the bridging W–C–N angles remain almost linear with maximum deviation from linearity of 2.4°.

In contrast to that in **1–5**, the Ln atom is eight coordinate and is surrounded by four cyano nitrogen atoms and four oxygen atoms from four water molecules. The coordination sphere of the Ln^{III} centre, {LnN₄O₄}, displays a slightly distorted square antiprism geometry (Figure 4). The sites of both faces are finished by four cyano nitrogen atoms and four oxygen atoms, respectively. The average Ln–N and Ln–O bond lengths both slightly decrease from **6** to **9** (on going from the Ho to Lu) because of systematic ionic radii contraction. The Ln–C1–N1 units are bent slightly with angles ranging from 167.8 to 169.6°. For **6–9**, the closest intramolecular Ln···W, Ln···Ln, and W···W distances are 5.806, 8.620 and 7.781 Å, respectively, and the shortest intermetallic distances between one layer and its closest neighbour (Ln···W, Ln···Ln and W···W) are 7.595, 7.761 and 7.761 Å, respectively. The O atom of one coordinated water molecule and the N2 atom of terminal CN group in neighbouring layers are connected through the relatively strong O–H···N hydrogen bonds with an average *d*_{O···N} distance of 7.761 Å.

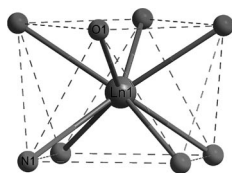


Figure 4. Coordination environment of **6–9**.

In summary, the structures of **1–9** comprise neutral corrugated layers consisting of 12-membered Ln₂W₂(CN)₄ puckered squares, which is similar to the 12-membered Ru₂Ln₂(CN)₄ squares observed in [{Ru(bpy)(CN)₄]₃{Ln(H₂O)₄]₂·*x*H₂O (Ln = Nd, Gd; *x* = 11 or 10, respectively).^[6]

The Phase Transformation in the Ln–W System

Powder samples of [Ln(H₂O)_{*n*}][W(CN)₈] (Ln = La, Pr, Nd, Sm, Eu, Gd, Tb, Ho, Er, Tm, Lu) were prepared by mixing aqueous solutions of (Bu₃NH)₃[W(CN)₈] and Ln(NO₃)₃·*n*H₂O. Powder XRD patterns (Figure S2) are in correspondence with those simulated from single-crystal structures, which reveals that the as-synthesized products are the expected materials. It is worth mentioning here that the powder XRD pattern of Tb(H₂O)₅[W(CN)₈] corresponds closely with that simulated from the single-crystal structure of Tb(H₂O)₅[Mo(CN)₈]^[5j] reported previously, indicating that the two complexes are isostructural.

Powder XRD patterns of [Ln(H₂O)_{*n*}][W(CN)₈] are shown in Figure 5. With increasing atomic number of Ln^{III} atoms from La to Tb, the diffraction patterns remain unchanged, which shows that the Ln–W systems (Ln = La, Ce, Pr, Nd, Sm, Eu, Gd, Tb) have the same lattice structure. Combining the powder data with the single-crystal struc-

tural analysis, we can speculate that the *n* value in [Ce(H₂O)_{*n*}][W(CN)₈] is five. With increasing atomic number (to Dy), some changes in the diffraction patterns were observed. A few peaks attributed to [Ln(H₂O)₅][W(CN)₈] disappear or reduce in intensity and some new peaks attributed to another uncertain phase emerge, which indicates the phase transformation. With atomic number increasing from Ho to Lu, [Ln(H₂O)₄][W(CN)₈] (Ln = Ho, Er, Tm, Lu) have the same lattice structures, which have been confirmed by single-crystal structures. We can conclude that a phase transformation occurs from [Ln(H₂O)₅][W(CN)₈] (Ln = La to Tb) to [Ln(H₂O)₄][W(CN)₈] (Ln = Ho to Lu) via [Dy(H₂O)_{*x*}][W(CN)₈] with increasing atomic number.

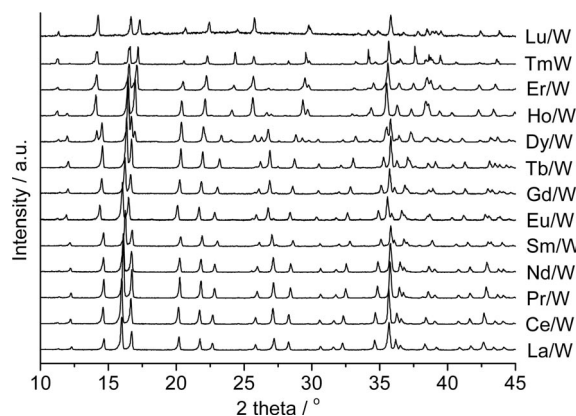


Figure 5. Powder XRD patterns of Ln(H₂O)_{*n*}[W(CN)₈].

TGA (Figure S3) and variable temperature powder XRD (Figures S4 and S5) results show that [Ln(H₂O)₅][W(CN)₈] (Ln = Sm, Eu, Gd, Tb) change reversibly to [Ln(H₂O)₄][W(CN)₈] with the loss of the first coordinated water molecule followed by the collapse of the framework structure with the loss of the remaining four coordinated water molecules on heating. Here we take complex **4** as an example. The TG result (Figure 6) reveals that one coordinated water molecule is lost at approximately 55 °C. The remaining four water molecules are lost gradually along with the collapse of framework, which can be confirmed by

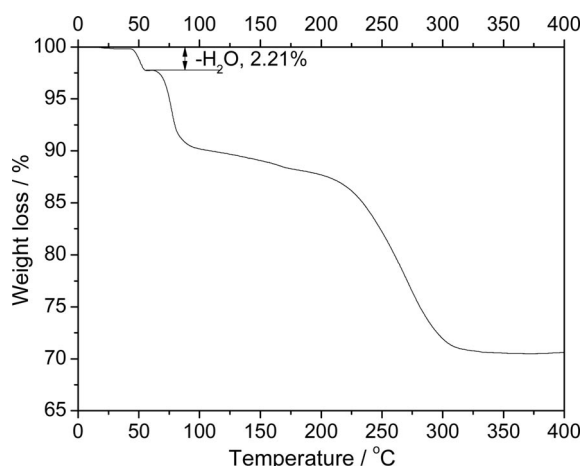


Figure 6. TG curve of **4**.

a variable temperature powder XRD experiment (Figure 7). In addition, the structure changes after **4** converts to [Eu(H₂O)₄][W(CN)₈], which reveals that the loss of the coordinated water molecule has an important impact on the structure of the framework. Interestingly, the process of this change is reversible (Figure 8). However, for [Ln(H₂O)₅][W(CN)₈] (Ln = La, Ce, Pr, Nd) and [Ln(H₂O)₄][W(CN)₈] (Ln = Ho, Er, Tm, Lu) the structures collapse directly when the coordinated water molecules are lost (Figures S3 and S4).

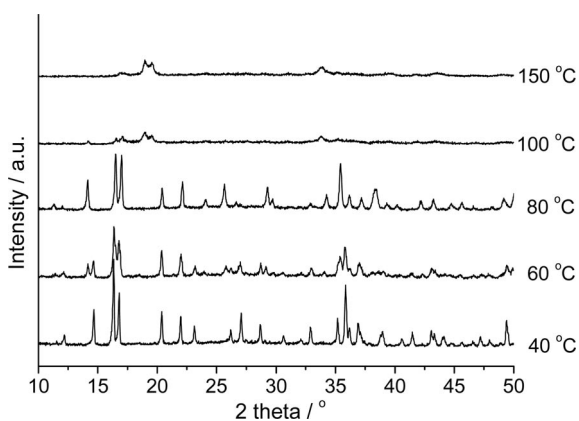


Figure 7. Variable temperature powder XRD patterns of **4**.

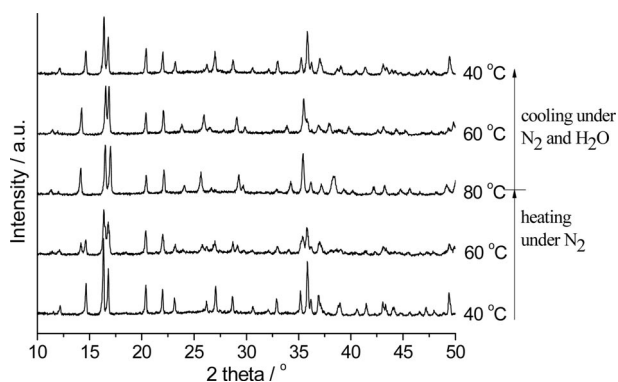


Figure 8. Variable temperature powder XRD patterns of **4** with sorption and desorption of water.

Conclusions

Two series of octacyanometallate-based complexes, Ln(H₂O)₅[W(CN)₈] [Ln = La(**1**), Pr(**2**), Nd(**3**), Eu(**4**), Gd(**5**)] and Ln(H₂O)₄[W(CN)₈] [Ln = Ho(**6**), Er(**7**), Tm(**8**), Lu(**9**)], have been synthesized and characterized structurally. The crystal structures of **1–9** have two-dimensional corrugated layers, in which the Ln^{III} and W^V centres are linked in an alternating fashion. TG and powder XRD results reveal the presence of a phase transformation in the Ln–W system with increasing atomic number of the Ln^{III} atoms.

Experimental Section

Materials: All chemicals and solvents were of analytical grade. (Bu₃NH)₃[W(CN)₈] was prepared according to the literature method.^[7] TG analysis revealed that the octacyanometallate precursor did not contain crystallized water molecules (Figure S1).

Syntheses of 1–9: Single crystals of **1–9** were prepared in the dark by slow diffusion of an acetonitrile solution (20 mL) containing Ln(NO₃)₃·*n*H₂O [Ln = La(**1**), Pr(**2**), Nd(**3**), Eu(**4**), Gd(**5**), Ho(**6**), Er(**7**), Tm(**8**), Lu(**9**)] (0.05 mmol) and (Bu₃NH)₃[W(CN)₈] (0.05 mmol). Orange crystals were formed over two to six weeks. **1:** C₈H₁₀LaN₈O₅W (620.97): calcd. C 15.47, H 1.62, N 18.05; found C 15.39, H 1.68, N 18.06. **2:** C₈H₁₀N₈O₅PrW (622.98): calcd. C 15.42, H 1.62, N 17.99; found C 15.52, H 1.55, N 18.02. **3:** C₈H₁₀N₈NdO₅W (626.31): calcd. C 15.34, H 1.61, N 17.89; found C 15.37, H 1.60, N 17.81. **4:** C₈H₁₀EuN₈O₅W (634.03): calcd. C 15.16, H 1.59, N 17.67; found C 15.13, H 1.66, N 17.72. **5:** C₈H₁₀GdN₈O₅W (639.32): calcd. C 15.03, H 1.58, N 17.53; found C 15.11, H 1.56, N 17.49. **6:** C₈H₈HoN₈O₄W (628.98): calcd. C 15.28, H 1.28, N 17.82; found C 15.31, H 1.26, N 17.86. **7:** C₈H₈ErN₈O₄W (631.31): calcd. C 15.22, H 1.28, N 17.75; found C 15.34, H 1.26, N 17.79. **8:** C₈H₈N₈O₄TmW (632.99): calcd. C 15.18, H 1.27, N 17.70; found C 15.14, H 1.30, N 17.65. **9:** C₈H₈LuN₈O₄W (639.02): calcd. C 15.04, H 1.26, N 17.54; found C 15.00, H 1.21, N 17.45. Powder samples were prepared by mixing aqueous solutions of (Bu₃NH)₃[W(CN)₈] (15 mL, 0.15 mmol) and Ln(NO₃)₃·2H₂O (Ln = La, Ce, Pr, Nd, Sm, Eu, Gd, Tb, Dy, Ho, Er, Tm, Lu) (15 mL, 0.15 mmol). C₈H₁₀N₈O₅WLa: C, 15.35; H, 1.59; N, 18.15. C₈H₁₀N₈O₅WCe: C, 15.43; H, 1.69; N, 18.10. C₈H₁₀N₈O₅WPr: C, 15.45; H, 1.66; N, 17.91. C₈H₁₀N₈O₅WNd: C, 15.40; H, 1.65; N, 17.97. C₈H₁₀N₈O₅WSm: C, 15.28; H, 1.62; N, 17.81. C₈H₁₀N₈O₅WEu: C, 15.15; H, 1.69; N, 17.64. C₈H₁₀N₈O₅WGd: C, 15.08; H, 1.59; N, 17.42. C₈H₁₀N₈O₅WTb: C, 15.04; H, 1.55; N, 17.54. C₈H₉N₈O_{4.5}WDy: C, 15.12; H, 1.42; N, 17.69. C₈H₈N₈O₄WHo: C, 15.32; H, 1.29; N, 17.86. C₈H₈N₈O₄WER: C, 15.18; H, 1.21; N, 18.88. C₈H₈N₈O₄WTm: C, 15.15; H, 1.27; N, 17.66. C₈H₈N₈O₄WLu: C, 15.10; H, 1.33; N, 17.51. Powder XRD patterns (Figure S2) of as-synthesized products correspond fully to those simulated from single-crystal structures (Figure S2), which reveals that highly pure products have been obtained.

Physical Measurements: Thermogravimetric (TG) analyses were carried out with a TA Instruments Hi-Res TGA 2950 analyzer to identify the approximate temperatures of guest water loss and thermal decomposition. The temperature was increased at a rate of 1 K/min from 294 K to 1053 K under a dry dinitrogen atmosphere with a 60 mL/min flow. Powder XRD patterns were collected with Cu-K_α radiation using a Shimadzu XRD-6000 diffractometer equipped with an Anton-Paar HTK 1200 stage for atmosphere and temperature control. Dehydration measurements were run under flowing dry dinitrogen with a heating rate of 1 K/min. For rehydration measurements the dinitrogen flow was saturated with water vapour by diverting the flow through a water bubbler.

X-ray Crystallographic Analysis: Diffraction data for **1–9** were collected with a Bruker Smart 1000 CCD equipped with Mo-K_α (λ = 0.71073 Å) radiation. Diffraction data analysis and reduction were performed with SMART, SAINT, and XPREP.^[8] Correction for Lorentz, polarization and absorption effects were performed with SADABS.^[9] Structures were solved by using the Patterson method with SHELXS-97^[10] and refined with SHELXL-97.^[11] All non-hydrogen atoms were refined with anisotropic thermal parameters. The H atoms bound to coordinated water molecules were located from difference maps and refined with a riding model. The crystallographic data and experimental details for the structural analyses

of 1–9 are summarized in Table S1. Selected bond lengths and angles are listed in Table S2. CCDC-716068 (1), -729451 (2), -698970 (3), -698971 (4), -698972 (5), -698973 (6), -698974 (7), -698975 (8) and -698976 (9) contain the supplementary crystallographic data for this paper. These data can be obtained free of charge from The Cambridge Crystallographic Data Centre via www.ccdc.cam.ac.uk/data_request/cif.

Supporting Information (see footnote on the first page of this article): Additional room-temperature powder XRD patterns, TG curves, variable-temperature powder XRD patterns and tables of crystallographic data and bond lengths and angles.

Acknowledgments

This work is supported by the Australian Research Council (DP0664834 and FF0561456), the University Natural Science Foundation of Jiangsu Province, China (No. 07KJB150030) and the Jiangsu Government Scholarship for Overseas Studies (China).

- [1] a) P. Przychodzeń, T. Korzeniak, R. Podgajny, B. Sieklucka, *Coord. Chem. Rev.* **2006**, *250*, 2234–2260; b) B. Sieklucka, R. Podgajny, P. Przychodzeń, T. Korzeniak, *Coord. Chem. Rev.* **2005**, *249*, 2203–2221; c) J. Larionova, S. Willemin, B. Donnadieu, B. Henner, C. Guérin, B. Gillon, A. Goujon, *J. Phys. Chem. Solids* **2004**, *65*, 677–691; d) B. Sieklucka, R. Podgajny, P. Przychodzeń, R. Kania, *C. R. Chim.* **2002**, *5*, 639–649; e) R. Garde, C. Desplanches, A. Bleuzen, P. Veillet, M. Verdaguer, *Mol. Cryst. Liq. Cryst.* **1999**, *334*, 587–595.
- [2] a) S. I. Ohkoshi, S. Ikeda, T. Hozumi, T. Kashiwagi, K. Hashimoto, *J. Am. Chem. Soc.* **2006**, *128*, 5320–5321; b) C. Mathonière, R. Podgajny, P. Guionneau, C. Labrugere, B. Sieklucka, *Chem. Mater.* **2005**, *17*, 442–449; c) T. Hozumi, K. Hashimoto, S. Ohkoshi, *J. Am. Chem. Soc.* **2005**, *127*, 3864–3869; d) J. M. Herrera, V. Marvaud, M. Verdaguer, J. Marrot, M. Kalisz, C. Mathonière, *Angew. Chem. Int. Ed.* **2004**, *43*, 5468–5471; e) Y. Arimoto, S. Ohkoshi, Z. J. Zhong, H. Seino, Y. Mizobe, K. Hashimoto, *J. Am. Chem. Soc.* **2003**, *125*, 9240–9241.
- [3] a) W. Kosaka, K. Imoto, Y. Tsunobuchi, S. Ohkoshi, *Inorg. Chem.* **2009**, *48*, 4604–4606; b) D. Pinkowicz, R. Podgajny, M. Bałanda, M. Makarewicz, B. Gawel, W. Łasocha, B. Sieklucka, *Inorg. Chem.* **2008**, *47*, 9745–9747; c) J. M. Herrera, P. Franz, R. Podgajny, M. Pilkington, M. Biner, S. Decurtins, H. Stoeckli-Evans, A. Neels, R. Garde, Y. Dromzée, M. Julve, B. Sieklucka, K. Hashimoto, S. Ohkoshi, M. Verdaguer, *C. R. Chim.* **2008**, *11*, 1192–1199; d) W. Kosaka, K. Hashimoto, S. Ohkoshi, *Bull. Chem. Soc. Jpn.* **2008**, *81*, 992–994; e) R. Podgajny, D. Pinkowicz, T. Korzeniak, W. Nitek, M. Rams, B. Sieklucka, *Inorg. Chem.* **2007**, *46*, 10416–10425; f) S. Ohkoshi, Y. Tsunobuchi, H. Takahashi, T. Hozumi, M. Shiro, K. Hashimoto, *J. Am. Chem. Soc.* **2007**, *129*, 3084–3085; g) H. Higashikawa, K. Okuda, J. Kishine, N. Masuhara, K. Inoue, *Chem. Lett.* **2007**, *36*, 1022–1023; h) J. R. Withers, D. F. Li, J. Triplet, C. Ruschman, S. Parkin, G. B. Wang, G. T. Yee, S. M. Holmes, *Inorg. Chem.* **2006**, *45*, 4307–4309; i) Y. Song, S. Ohkoshi, Y. Arimoto, H. Seino, Y. Mizobe, K. Hashimoto, *Inorg. Chem.* **2003**, *42*, 1848–1856; j) Z. J. Zhong, H. Seino, Y. Mizobe, M. Hidai, M. Verdaguer, S. Ohkoshi, K. Hashimoto, *Inorg. Chem.* **2000**, *39*, 5095–5101.
- [4] a) J. H. Lim, J. H. Yoon, H. C. Kim, C. S. Hong, *Angew. Chem. Int. Ed.* **2006**, *45*, 7424–7426; b) Y. Song, P. Zhang, X. M. Ren, X. F. Shen, Y. Z. Li, X. Z. You, *J. Am. Chem. Soc.* **2005**, *127*, 3708–3709.
- [5] a) I. V. Typilo, O. A. Sereda, H. Stoeckli-Evans, R. E. Gladyshevskii, D. I. Semenyshyn, *Russ. J. Coord. Chem.* **2009**, *35*, 920–924; b) I. V. Typilo, O. A. Sereda, D. I. Semenyshyn, H. Stoeckli-Evans, R. E. Gladyshevskii, *Pol. J. Chem.* **2009**, *83*, 339–344; c) O. A. Sereda, G. Stöckli-Evans, I. V. Typilo, D. I. Semenyshyn, R. E. Gladyshevskii, *Russ. J. Coord. Chem.* **2009**, *35*, 15–18; d) S. L. Ma, S. Ren, Y. Ma, D. Z. Liao, *J. Chem. Sci.* **2009**, *121*, 421–427; e) S. L. Ma, S. Ren, *J. Inorg. Organomet. Polym.* **2009**, *19*, 382–388; f) E. Chelebaeva, J. Larionova, Y. Guari, R. A. S. Ferreira, L. D. Carlos, F. A. A. Paz, A. Trifonov, C. Guérin, *Inorg. Chem.* **2009**, *48*, 5983–5995; g) S. Tanase, M. Evangelisti, L. J. de Jongh, J. M. M. Smits, R. de Gelder, *Inorg. Chim. Acta* **2008**, *361*, 3548–3554; h) S. Tanase, L. J. de Jongh, F. Prins, M. Evangelisti, *ChemPhysChem* **2008**, *9*, 1975–1978; i) S. L. Ma, Y. Ma, D. Z. Liao, S. P. Yan, Z. H. Jiang, G. L. Wang, *Chin. J. Inorg. Chem.* **2008**, *24*, 1290–1293; j) E. Chelebaeva, J. Larionova, Y. Guari, R. A. S. Ferreira, L. D. Carlos, F. A. A. Paz, A. Trifonov, C. Guérin, *Inorg. Chem.* **2008**, *47*, 775–777; k) P. Przychodzeń, R. Pełka, K. Lewiński, J. Supel, M. Rams, K. Tomala, B. Sieklucka, *Inorg. Chem.* **2007**, *46*, 8924–8938; l) F. Prins, E. Pasca, L. J. de Jongh, H. Kooijman, A. L. Spek, S. Tanase, *Angew. Chem. Int. Ed.* **2007**, *46*, 6081–6084; m) W. Kosaka, K. Hashimoto, S. Ohkoshi, *Bull. Chem. Soc. Jpn.* **2007**, *80*, 2350–2356; n) Z. X. Wang, X. F. Shen, J. Wang, P. Zhang, Y. Z. Li, E. N. Nfor, Y. Song, S. Ohkoshi, K. Hashimoto, X. Z. You, *Angew. Chem. Int. Ed.* **2006**, *45*, 3287–3291; o) S. Tanase, F. Prins, J. M. M. Smits, R. de Gelder, *CrystEngComm* **2006**, *8*, 863–865; p) P. Przychodzeń, K. Lewiński, R. Pełka, M. Bałanda, K. Tomala, B. Sieklucka, *Dalton Trans.* **2006**, 625–628; q) S. Ikeda, T. Hozumi, K. Hashimoto, S. Ohkoshi, *Dalton Trans.* **2005**, 2120–2123; r) T. Hozumi, S. Ohkoshi, Y. Arimoto, H. Seino, Y. Mizobe, K. Hashimoto, *J. Phys. Chem. B* **2003**, *107*, 11571–11574.
- [6] G. M. Davies, S. J. A. Pope, H. Adams, S. Faulkner, M. D. Ward, *Inorg. Chem.* **2005**, *44*, 4656–4665.
- [7] L. D. C. Bok, J. G. Leipoldt, S. S. Basson, *Z. Anorg. Allg. Chem.* **1975**, *415*, 81–83.
- [8] SMART, SAINT and XPREP: Area Detector Control and Data Integration and Reduction Software, Bruker Analytical X-ray Instruments Inc., Madison, Wisconsin, USA, **1995**.
- [9] G. M. Sheldrick, SADABS: Empirical Absorption and Correction Software, University of Göttingen, Göttingen, Germany, **1999**.
- [10] G. M. Sheldrick, SHELXS-97: Programs for Crystal Structure Solution, University of Göttingen, Göttingen, Germany, **1997**.
- [11] G. M. Sheldrick, SHELXL-97: Programs for the Refinement of Crystal Structures, University of Göttingen, Göttingen, Germany, **1997**.

Received: March 21, 2010
Published Online: July 1, 2010